

## Article

# Middle Latitude Geomagnetic Disturbances Caused by Hall and Pedersen Current Circuits Driven by Prompt Penetration Electric Fields

Takashi Kikuchi <sup>1,\*</sup>, Kumiko K. Hashimoto <sup>2</sup>, Takashi Tanaka <sup>3</sup>, Yukitoshi Nishimura <sup>4</sup> and Tsutomu Nagatsuma <sup>5</sup>

<sup>1</sup> Institute for Space-Earth Environmental Research, Nagoya University, Furo-cho, Chikusa-ku, Nagoya 464-8601, Japan

<sup>2</sup> School of Agriculture, Kibi International University, 370-1, Shichi-Sareo, Minamiawaji 656-0484, Japan; hashi@kiui.ac.jp

<sup>3</sup> International Center for Space Weather Science and Education, Kyushu University, Fukuoka 819-0395, Japan; tatanaka@serc.kyushu-u.ac.jp

<sup>4</sup> Center for Space Physics, Boston University, Boston, MA 02215, USA; toshi16@bu.edu

<sup>5</sup> National Institute of Information and Communications Technology, Tokyo 184-0015, Japan; tnagatsu@nict.go.jp

\* Correspondence: kikuchi@isee.nagoya-u.ac.jp

**Abstract:** The prompt penetration electric field (PPEF) drives the DP2 currents composed of the two-cell Hall current vortices surrounding the Region-1 field-aligned currents (R1FACs), and the zonal equatorial electrojet (EEJ, Cowling current) at the dayside equator, which is connected to the R1FACs by the Pedersen currents at middle latitudes. The midlatitude  $H$ - and  $D$ -components of the disturbance magnetic field are caused by the DP2 currents, as well as by the magnetospheric currents, such as magnetopause currents, FACs, ring currents, and so on. If the DP2 current is the major source for the midlatitude geomagnetic disturbances,  $H$  and  $D$  are supposed to be caused by the Hall and Pedersen currents, respectively. The  $H$ - $D$  correlation would be negative in both morning and afternoon sectors, and  $H/D$ - $EEJ$  correlation would be negative/positive in the morning and positive/negative in the afternoon. We picked out 39 DP2 events in the morning and 34 events in the afternoon from magnetometer data at Paratunka, Russia (PTK, 45.58° N geomagnetic latitude (GML)), which are characterized by negative  $H$ - $D$  correlation with correlation coefficient ( $cc$ )  $< -0.8$ . We show that the midlatitude  $H/D$  is highly correlated with  $EEJ$  at Yap, Micronesia (0.38° S GML) in the same local time zone, meeting the Pedersen–Cowling current circuit between midlatitude and equator in the DP2 current system. Using the global simulation, we confirmed that the ionospheric currents with north–south direction at midlatitude is the Pedersen currents developing concurrently with the Cowling current. We suggest that the negative  $H$ - $D$  correlation provides a clue to detect the PPEF when magnetometers are available at middle latitudes.

**Keywords:** DP2 magnetic fluctuation; middle latitude; Hall and Pedersen currents; Pedersen–Cowling current circuit; equatorial electrojet; global simulation



**Citation:** Kikuchi, T.; Hashimoto, K.K.; Tanaka, T.; Nishimura, Y.; Nagatsuma, T. Middle Latitude Geomagnetic Disturbances Caused by Hall and Pedersen Current Circuits Driven by Prompt Penetration Electric Fields. *Atmosphere* **2022**, *13*, 580. <https://doi.org/10.3390/atmos13040580>

Academic Editor:  
Christine Amory-Mazaudier

Received: 24 February 2022

Accepted: 31 March 2022

Published: 4 April 2022

**Publisher's Note:** MDPI stays neutral with regard to jurisdictional claims in published maps and institutional affiliations.



**Copyright:** © 2022 by the authors. Licensee MDPI, Basel, Switzerland. This article is an open access article distributed under the terms and conditions of the Creative Commons Attribution (CC BY) license (<https://creativecommons.org/licenses/by/4.0/>).

## 1. Introduction

The prompt penetration electric field (PPEF) has been detected by the magnetometers deployed from high latitudes to the equator during the quasi-periodic DP2 magnetic fluctuations with periods of 30–60 min [1–6]. The equivalent currents are composed of two-cell current vortices at high and middle latitudes and zonal currents at the dayside dip equator [1,2]. The DP2 currents at high and middle latitudes were shown to be the Hall currents, as derived from the EISCAT radar and IMAGE magnetometer observations [3]. The DP2 magnetic variations are well correlated with fluctuations in the interplanetary magnetic field (IMF) [2,4] and solar wind dynamic pressure [7]. The DP2 Hall current

vortices are driven by the dawn-to-dusk convection electric field generated by the dynamo activated by the southward IMF [8] and/or by solar wind dynamic pressure [9,10].

The R1FACs flow into the polar ionosphere and then to the equatorial ionosphere via the midlatitude ionosphere to achieve the polar-equatorial current circuit [3]. The equatorial currents, i.e., *EEJ* (equatorial electrojet) are the Pedersen currents enhanced by the Cowling conductivity, such that the primary Pedersen currents are intensified by the Hall currents due to the vertical polarization electric field created by the primary electric field in the vertical Hall-Pedersen current circuit [11,12]. The Cowling currents are supplied by the Pedersen currents from the FACs via the midlatitude ionosphere, completing the Pedersen-Cowling current circuit, as well as the two-cell Hall current vortices as schematically shown in Figure 1 (modified Figure 9 of Kikuchi et al. [3]).

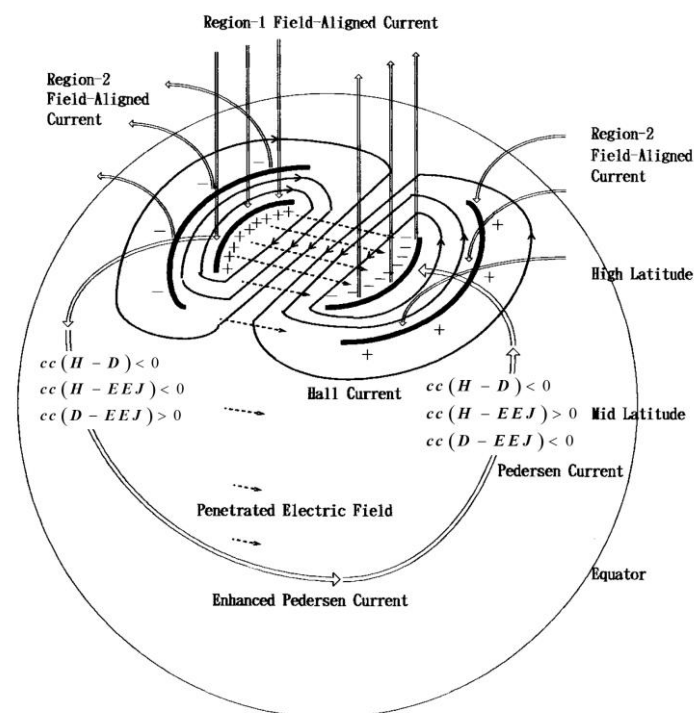


**Figure 1.** Schematic diagram of the DP2 ionospheric currents modified from Figure 9 of Kikuchi et al. [3]. Two-cell Hall currents surround the Region-1 field-aligned currents at high and middle latitudes. The R1FAC drives a current circuit with midlatitude Pedersen current and equatorial Cowling current (enhanced Pedersen current, *EEJ*).  $cc(H-D)$ ,  $cc(H-EEJ)$ , and  $cc(D-EEJ)$  refer to correlations between midlatitude *H* and *D* and correlations between *H/D* and *EEJ*.

Thus, the equatorial ionosphere works as if it is a sensitive antenna to the electric field and currents originating in the magnetosphere. In fact, *EEJ* has been extensively used as a detector of the PPEF of the preliminary impulse (PI) and main impulse (MI) of the geomagnetic sudden commencement (SC) ([13] and references therein), Pc5 pulsations [14,15] and Pi2 pulsations [16,17], substorm and storms [18–23] and SAPS (subauroral polarization stream) [24,25]. *EEJ* is caused not only by the PPEF but also by solar flares and disturbance dynamo electric fields [26]. Even during quiet times, *EEJ* is caused by zonal wind in the ionosphere and tidal motion of the thermosphere [27,28]. Since the transmission of the electric field and currents from the foot of R1FACs to *EEJ* is almost instantaneous [29], the DP2 fluctuations are well correlated between high latitude and equator with the correlation coefficient of 0.9 within the temporal resolution of 25 s [3]. The PPEF transmitted with the DP2 currents are observed by the HF Doppler sounders at middle latitudes during SC and storm/substorms [30–33] and at the equator [34]. Furthermore, the PPEF is transmitted from the ionosphere upward into the inner magnetosphere as observed by spacecrafts [35,36].

The instantaneous transmission from high latitude to the equator can be proved by using the onset time of PI of SC, which can be determined within the resolution of 10 s [31,37,38]. The instantaneous achievement of the polar-equatorial current circuit is due to the zeroth-order transverse magnetic (TM<sub>0</sub>)/transverse electromagnetic (TEM) mode waves propagating at the speed of light in the Earth–ionosphere waveguide/transmission line [29,39,40]).

As described above, the equatorial magnetometers are a powerful tool for detecting the PPEF, but the number of stations and periods of operation are limited compared to those at middle latitudes where many magnetometers have been operated on a global scale and over long periods (WDC for Geomagnetism, Kyoto, Japan). Therefore, it is of great concern whether magnetometers deployed at midlatitudes are capable of detecting the PPEF. If this method works well, we can follow the evolution of the PPEF at any stage of ongoing space weather disturbances and also in the post-event analyses of past major storms.

The midlatitude magnetic fields on the ground are under strong influence of the DP2 currents, but superimposed by significant effects due to magnetospheric currents, such as the magnetopause current, ring currents, FACs and so on. Sibeck et al. [7] reported that quite a few DP2 events at the equator are caused by the solar wind dynamic pressure, which would predict that midlatitude DP2 is caused by both the ionospheric currents and magnetopause currents. The midlatitude SC has been known to be caused by ionospheric PI and MI currents, as well as by magnetopause currents [13]. The PI of SC is also under strong influence of FACs in winter when the ionospheric conductivity is low [41]. On the other hand, the *D*-component of the magnetic field at middle latitudes have been attributed to the ionospheric Pedersen currents flowing in north–south direction (Figure 1), which results in opposite polarity in the morning and afternoon as observed in the SC [42], substorm [21], and storm [33]. Imajo et al. [17] showed that *D* of Pi2 pulsations changes its polarity across the terminator, meeting the Pedersen currents on the sunlit side and FACs on the dark side.

Thus, midlatitude *H* and *D* are caused not only by the ionospheric currents driven by the PPEF but also by magnetospheric currents, which can make it difficult to detect the PPEF with midlatitude magnetometers. However, if midlatitude *H* and *D* are caused solely by the ionospheric Hall and Pedersen currents, respectively, we would be able to obtain information about the PPEF from negative correlations between *H* and *D* in both the morning and afternoon as deduced from the DP2 current system in Figure 1. We further expect that correlations between midlatitude *H* and *EEJ* are negative/positive in the morning/afternoon and correlations between midlatitude *D* and *EEJ* are positive/negative in the morning/afternoon.

The purpose of the present paper is to prove that the PPEF can be detected by midlatitude magnetometer, using high negative correlations between *H* and *D*. For this purpose, we picked out 39 DP2 events with correlation coefficient,  $cc(H-D) < -0.8$  in the morning and 34 events with the same criteria in the afternoon, using magnetometer data from Paratunka, Russia (PTK, 45.58° GML). To confirm the selected DP2 events being caused by the PPEF, we examined DP2 current circuit conditions, i.e., high correlations between mid-latitude *H/D* and *EEJ* which is defined as difference between *H* at Okinawa, Japan (OKI, 16.95° GML) and Yap, Micronesia (YAP, 0.51° GML) in the same local time zone (Table 1). We use “*EEJ*” for *H* due to the equatorial electrojet and “Cowling current” for the current circuit, such as the Pedersen–Cowling current circuit. Hereafter, *H* and *D* at PTK are referred to as *PTKH* and *PTKD* and the same abbreviations are applied to other stations. The correlation coefficients between variables are referred to as  $cc(PTKH-D)$ ,  $(PTKD-EEJ)$ ,  $(PTKD-OKID)$ , and so on. In Sections 2 and 3, we show that selected *PTKH* and *PTKD* agree with the Hall current vortices at midlatitude and the Pedersen–Cowling current circuit from midlatitude to the equator, respectively. In Section 4, we show that the R1FAC dynamo supplies the Hall and Pedersen currents at midlatitude and equatorial Cowling currents, using the global MHD (magnetohydrodynamics) simulation [43].

**Table 1.** List of the National Institute of Communications and Technology (NICT) space weather monitoring magnetometer stations.

STATION	COUNTRY	GEOGRAPHIC (deg)		GEOMAGNETIC (deg)		MLT UT+
		Latitude	Longitude	Latitude	Longitude	
PTK, Paratunka	Russia	52.94° N	158.25° E	45.58° N	221.13° E	10.6
OKI, Okinawa	Japan	26.78° N	128.25° E	16.95° N	198.69° E	8.4
YAP, Yap	Micronesia	9.49° N	138.09° E	0.51° N	209.45° E	9.1

**2. DP2 Events in the Morning Sector (0630-1030MLT)**

We have analyzed 39 DP2 events observed at PTK in the morning (20-24 UT, 0630-1030 MLT), with the amplitude of  $D$  as  $dD > 15\text{nT}$  and the correlation coefficients between  $PTKH$  and  $PTKD$  as  $cc(PTKH-D) < -0.8$ . To calculate the correlation coefficients between periodic variations of two variables, we removed background gradual variations by applying moving average with the high-pass window of 60 min. Therefore, DP2 variations with periods  $< 60$  min are picked out.

Figure 2 shows four DP2 events recorded at PTK, OKI, and YAP ( $EEJ$ ), where  $PTKH$ ,  $OKIH$  and  $EEJ$  are shown with solid lines and  $PTKD$ ,  $OKID$ , and  $YAPH$  with dotted lines. Plots of  $OKIH$  and  $OKID$  are magnified by three to increase the visibility of small amplitude of  $OKIH$  and  $OKID$ , which does not affect the correlation coefficients. The small amplitude at OKI is due to the geometrical attenuation of the PPEF propagating from the polar ionosphere [3].

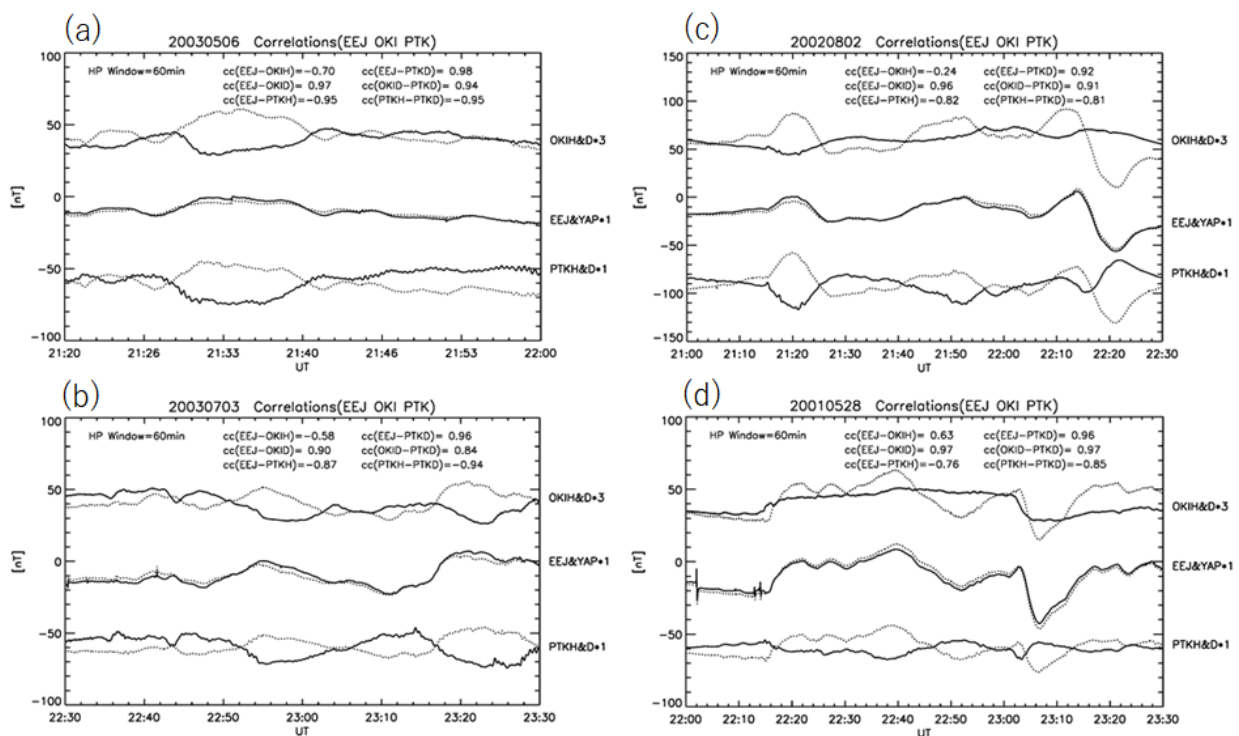


**Figure 2.** DP2 magnetic fluctuations recorded in  $H$  and  $D$  at PTK and OKI in the morning (0630-1030 MLT), denoted with  $PTKH$  (solid curve),  $PTKD$  (dotted curve),  $OKIH$  (solid curve), and  $OKID$  (dotted curve).  $OKIH$  and  $OKID$  are multiplied by three for better visibility. At the equator,  $EEJ$  (solid curve) and  $YAPH$  (dotted curve) are shown. The correlation coefficients between two variables are shown with  $cc$  in the frame. (a–d) are used for reference in the text.

In Figure 2a,b, the correlation between *PTKH* and *PTKD* is excellent as  $cc(PTKH-D) = -0.95$  and  $-0.94$ , which agrees with the Hall and Pedersen currents driven by the PPEF, as depicted in Figure 1. The correlation between *PTKH* and *EEJ* is also excellent as  $cc(PTKH-EEJ) = -0.95$  and  $-0.87$ . The negative correlation indicates that *PTKH* is caused by the clockwise Hall current in the morning with no significant effects of the magnetospheric currents. If *PTKH* was caused by magnetospheric currents, we would expect positive correlations as seen at low latitude and equator during the SC [13] and solar wind pressure-driven DP2 [7]. Moreover, the correlations,  $cc(PTKD-EEJ) = 0.98$  and  $0.96$  and  $cc(OKID-EEJ) = 0.97$  and  $0.90$  prove that the Pedersen–Cowling current circuit is achieved from PTK to the equator via OKI. It is to be noted that the Hall currents extend to OKI as inferred from  $cc(OKIH-EEJ) = -0.70$  (Figure 2a). The smaller  $cc(OKIH-EEJ)$  than  $cc(PTKH-EEJ)$  may indicate more contribution of magnetospheric current effects on *OKIH*.

Figure 2c,d show that the correlation between the *PTKH* and *PTKD* is  $cc(PTKH-D) = -0.81$  and  $-0.85$ , which agrees with the Hall and Pedersen currents driven by the PPEF. The smaller  $cc$  may be due to the magnetospheric current effects superimposed on *PTKH*. The correlation between the *PTKH* and *EEJ* is  $cc(PTKH-EEJ) = -0.82$  and  $-0.76$ , indicating that *PTKH* is caused by the clockwise Hall current in the morning, probably with some effects of the magnetospheric currents. On the other hand, high correlations,  $cc(PTKD-EEJ) = 0.92$  and  $0.96$  and  $cc(OKID-EEJ) = 0.96$  and  $0.97$  indicate that *PTKD* and *OKID* are caused almost only by the Pedersen currents connecting to *EEJ*. The positive correlation  $cc(OKIH-EEJ) = 0.63$  in the event (d) indicates dominant magnetospheric current effects on *OKIH*. It is remarkable that, even in this case,  $cc(OKID-EEJ) = 0.97$  indicates exclusive role of the Pedersen currents on *OKID*.

We calculated correlation coefficients between two variables selected from *PTKH/D*, *OKIH/D* and *EEJ* of 39 DP2 events. Figure 3 (top panel) shows correlation coefficients between *PTKD* and other variables,  $cc(PTKH-D)$ ,  $cc(PTKD-EEJ)$ ,  $cc(PTKD-OKIH)$ , and  $cc(PTKD-OKID)$ . All  $cc(PTKH-D)$  are between  $-1$  and  $-0.8$  from the selection criteria and most of  $cc(PTKD-EEJ)$  and  $cc(PTKD-OKID)$  are  $> 0.9$  with some scatterings. These high-correlation coefficients match the clockwise Hall current vortex and southward Pedersen–eastward Cowling current circuit from PTK to YAP over OKI, as depicted in Figure 1. In particular, the high value of  $cc(PTKD-OKID)$  indicates that *D* is caused by the Pedersen currents even at low latitudes as OKI. This result suggests that the midlatitude *D* provides us with a clue to estimate the PPEF. On the other hand, the plots of  $cc(PTKD-OKIH)$  scatters between  $-0.8$  and  $+0.8$ , which may indicate significant contribution of non-ionospheric currents, i.e., magnetospheric currents on *OKIH*.

Figure 3 (bottom panel) shows box plots of all the correlation coefficients, displaying the minimum, lower quartile, median, upper quartile, and maximum with outliers (dots). The average value is indicated by  $x$  inside the box. The lower/upper quartile is the median of the data points below/above the median. Therefore, 50% of the events are inside the box and 75% above the lower quartile. The median values of  $cc(PTKH-EEJ)$ ,  $cc(PTKD-EEJ)$ , and  $cc(OKID-EEJ)$  are  $-0.809$ ,  $0.926$ , and  $0.923$ , respectively, under the condition of the median value of  $cc(PTKH-D) = -0.863$ . These correlation coefficients match the Hall current and Pedersen–Cowling current circuits as shown in Figure 1.

In contrast, the correlations between *OKIH* and other variables are  $-0.3 \sim +0.4$ , which may indicate contamination of non-ionospheric currents such as the magnetopause currents, FACs and so on. It is interesting to note that  $cc(OKIH-EEJ)$  is negative in about 75% of the events. If *OKIH* was caused by the ionospheric Pedersen currents driven by the PPEF, *OKIH* should be in the same direction as *EEJ*, resulting in positive  $cc(OKIH-EEJ)$ . Therefore, the negative  $cc(OKIH-EEJ)$  may indicate an extension of the Hall currents to low latitude of  $16.87^\circ$  GML and the remaining 25% of the events may be dominated by magnetospheric current effects. On the other hand,  $cc(PTKH-EEJ)$  is negative in all the events, indicating that the DP2 Hall current effects are dominant at PTK, even when the magnetospheric current effects are dominant at OKI. The latitudinal dependence of the contribution of the DP2 currents is due to the geometrical attenuation of PPEF during its propagation

from the polar ionosphere to the equator [29]. In Section 4, we will show that the global simulation reproduced extension of the Hall currents to PTK and OKI, which explains negative  $cc(PTKH-EEJ)$  and  $cc(OKIH-EEJ)$  in the morning.

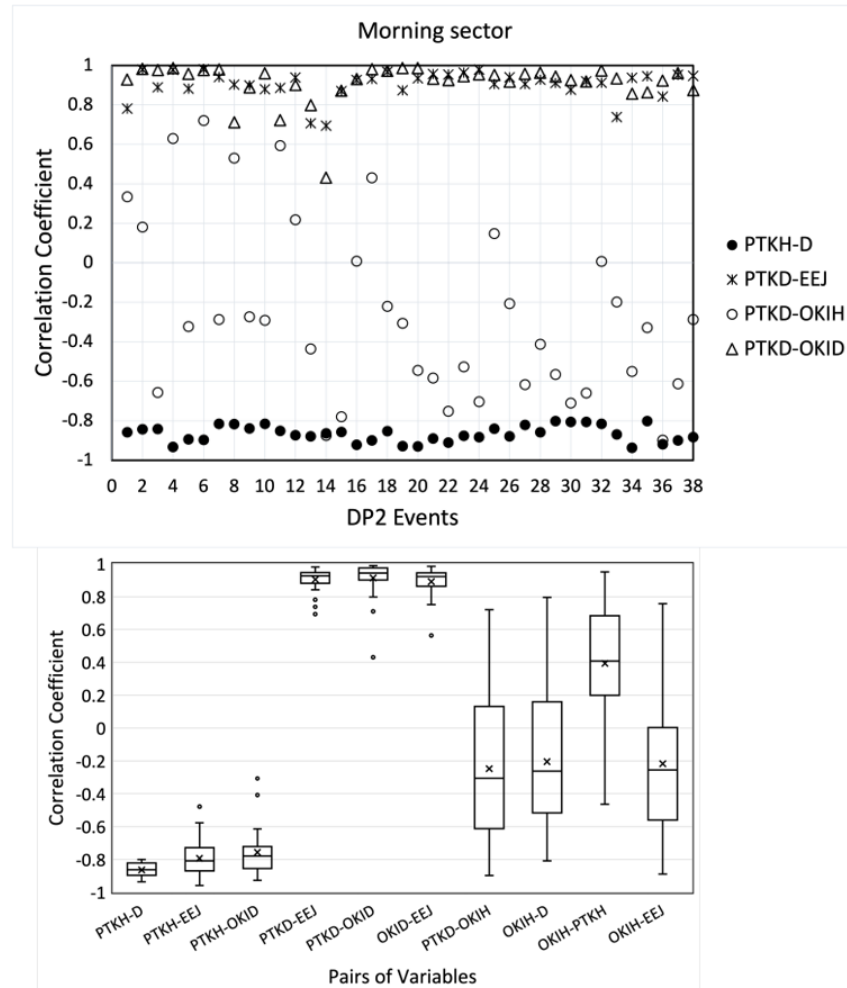


**Figure 3.** (top) Scatter plots of correlation coefficients between *PTKD* and other variables of 39 DP2 events in the morning sector;  $cc(PTKH-D)$ ,  $cc(PTKD-EEJ)$ ,  $cc(PTKD-OKIH)$ , and  $cc(PTKD-OKID)$ . (bottom) Box plots of all the correlation coefficients between two variables, composed of the minimum, lower quartile, median, upper quartile, and maximum with outliers (dots). The average value is indicated by x inside the box.

### 3. DP2 Events in the Afternoon (1330–1730MLT)

We have analyzed 34 DP2 events observed at PTK in the afternoon (0300–0700 UT, 1330–1730 MLT), with the amplitude of  $dD > 10nT$  and the correlation coefficients between  $H$  and  $D$  being  $cc(PTKH-D) < -0.8$ . The low threshold of  $D$  is used because the intensity of the DP2 current is estimated to be low in the afternoon, as will be explained in Section 4. To calculate the correlation coefficients between two variables, we applied the moving average same as used for the events in the morning.

Figure 4a–d show typical DP2 events with high correlations as  $cc(PTKH-D) = -0.89, -0.89, -0.85, -0.92$ , which matches the DP2 current circuit composed of the Hall and Pedersen currents (Figure 1). The correlation between the *PTKH* and *EEJ* is positive as  $cc(PTKH-EEJ) = 0.96, 0.98, 0.92, 0.92$ , matching the counter-clockwise Hall currents and eastward *EEJ*. The correlations,  $cc(OKIH-EEJ) = 0.87, 0.87, 0.93, 0.80$  may indicate the DP2 Hall currents extending over to OKI. The correlations,  $cc(PTKD-EEJ) = -0.81, -0.86, -0.80, -0.92$  agree with the Pedersen current circuit from PTK to the equator, while  $cc(OKID-EEJ) = -0.24, -0.93, -0.81, -0.14$  may indicate less contribution of the

Pedersen currents at OKI in the afternoon sector, where the Pedersen currents flow in wider local time zone than in the morning sector, as will be discussed using the global simulation.

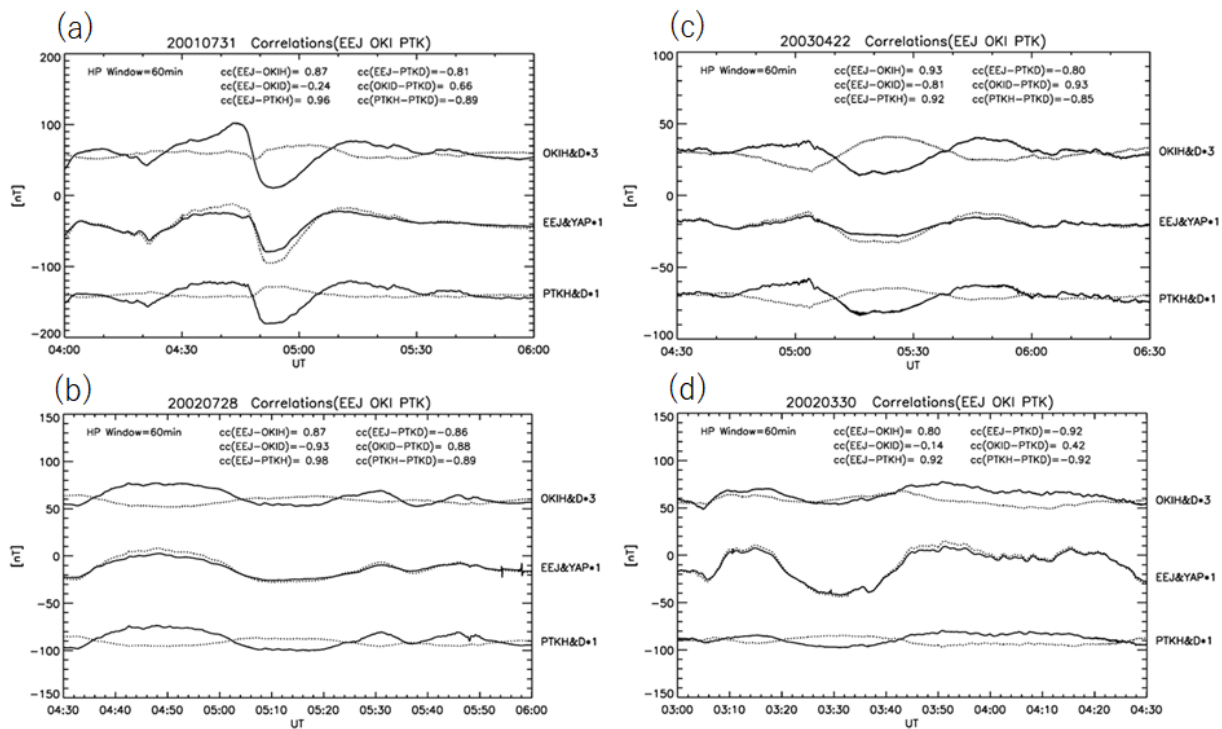


**Figure 4.** DP2 magnetic perturbations recorded in the afternoon (1330–1730 MLT). The format is the same as in Figure 1. (a–d) are used for reference in the text.

Figure 5 shows the correlation coefficients in the same format as in Figure 3. The median values of  $cc(PTKH-EEJ)$  and  $cc(PTKD-EEJ)$  are 0.855 and  $-0.830$ , which matches the Hall current and Pedersen-Cowling current circuits (Figure 1). On the other hand, the median values of  $cc(OKIH-D)$  and  $cc(OKID-EEJ)$  are  $-0.451$  and  $-0.522$ , respectively. The poor correlations compared to  $cc(PTKD-EEJ)$  may be due to low intensity of the Pedersen currents at low latitudes. One of the reasons for the low Pedersen current is the expansion of the electric potential and currents beyond the dusk terminator, as will be shown with the global simulation (Section 4). The expansion of the electric potentials beyond the terminator is related to the evening anomaly of the PPEF of which direction is the same as in the day [44]. The lower  $cc(PTKD-EEJ)$  in the afternoon than in the morning may be due to overwhelming FAC effects on  $PTKD$  like the Pi2 pulsations [17]. Imajo et al. [17] showed that the phase of the Pi2 in  $D$ -component changes its polarity 2–3 h before sunset, while 0.5 h after sunrise. As a result, the midlatitude  $D$  in the afternoon is less sensitive to the PPEF than in the morning sector, although the midlatitude  $H$  is sensitive to the PPEF. In contrast,  $cc(OKIH-PTKH) = 0.9075$  and  $cc(OKIH-EEJ) = 0.818$  in the afternoon, much higher than  $cc(OKIH-PTKH) = 0.409$  and  $cc(OKIH-EEJ) = -0.256$  in the morning sector. As will be discussed later, the Hall currents tend to increase  $PTKH$  and  $OKIH$  in the afternoon, but decrease them in the morning, if  $EEJ$  increases. The positive/negative magnetic fields due to the Hall currents may have resulted in higher/lower correlation coefficients in the afternoon/morning sector.

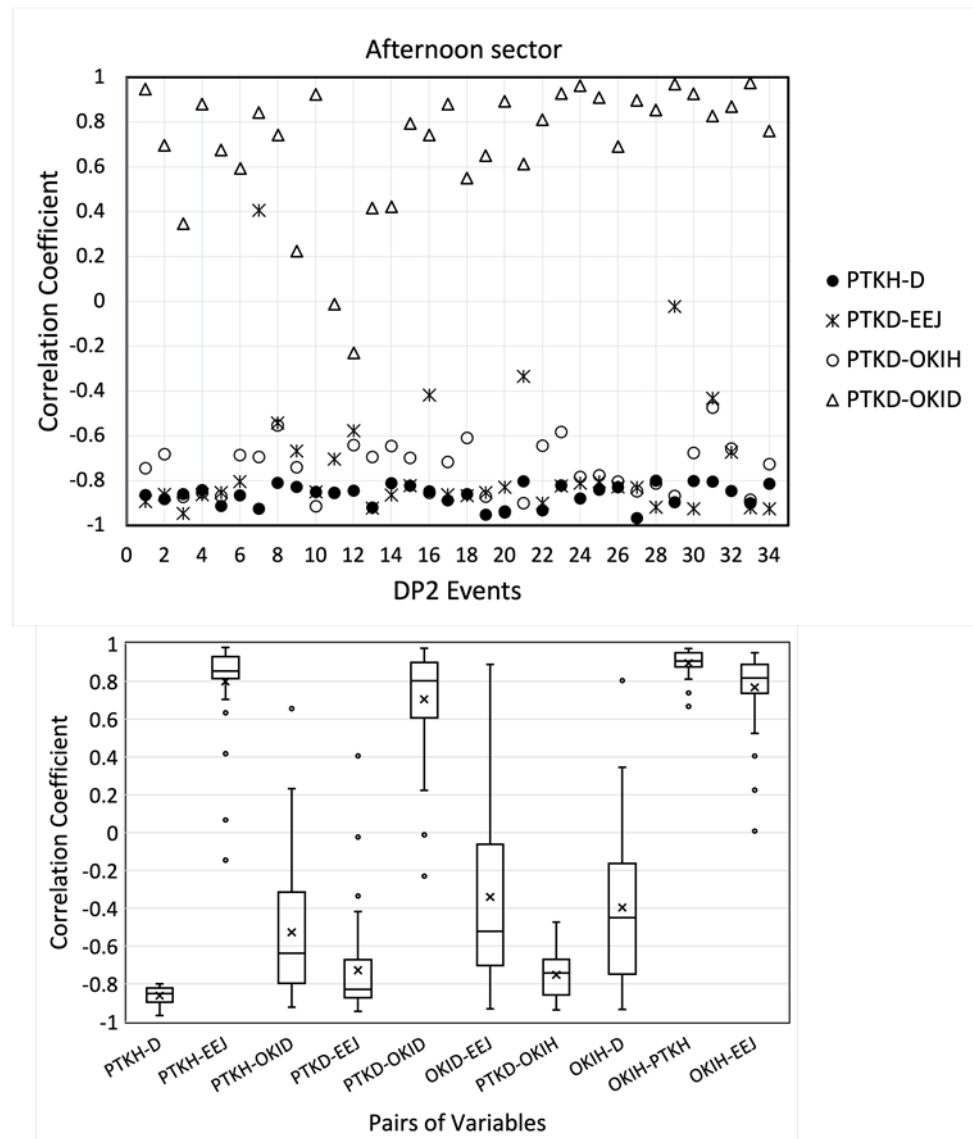


**Figure 5.** (top) Scatter plots of correlation coefficients and (bottom) box plots of all the correlation coefficients between two variables in the same format as in Figure 3.

#### 4. Reproduction of Hall and Pedersen-Cowling Currents

To confirm the Hall and Pedersen-Cowling current circuit scenario, we reproduced the Hall and Pedersen currents at  $45.6^\circ$  magnetic latitude (MLAT) and  $17.0^\circ$  MLAT, as well as the Pedersen (Cowling) current at the equator ( $0.0$  MLAT), using the REPPU (Reproduce Plasma Universe) simulation code [43]. The REPPU model uses the total variation diminishing finite volume scheme and the ionosphere is located at the inner simulation boundary of  $2.6$  Re with the Pedersen and Hall conductivities. The ionospheric electric potentials are calculated with the field-aligned currents as an input from the magnetosphere. At the simulation boundary upstream in the solar wind, the IMF  $B_z$  changes from  $+5$  nT to  $-5$  nT and solar wind speed from  $372$  to  $500$  km/s in the form of a step function. The solar wind density and IMF  $B_y$  are constant  $5/\text{cc}$  and  $2.5$  nT, respectively. The REPPU model has succeeded to reproduce the magnetosphere-ionosphere currents of the substorm [45] and polar-equatorial ionospheric currents of the substorm overshielding [46].

Figure 6 shows time evolution of the Hall and Pedersen currents at the latitude of PTK ( $45.6^\circ$  MLAT) with eastward (panels (a) and (b)) and northward (panels (c) and (d)) directions. The vertical axis is the magnetic local time (MLT) and horizontal axis is the

simulation time (hh:mm). The solar wind pressure activates dynamos of PI and MI of SC [9,10], and then the southward IMF activates the dynamo of the convection electric field and R1FACs [8,43]. Figure 6a shows that the eastward/westward Hall currents of the PI are created in the morning/afternoon for the first few minutes, followed by reverse currents of the MI for the next several minutes. The MI currents are further followed by DP2 currents driven by the R1FAC dynamo, continuing for 1 h. We focus our attention to the DP2 currents of which directions are westward in the morning and eastward in the afternoon and evening. Figure 6b shows the Pedersen currents of which direction is eastward in the day, while the current density is lower than the Hall current. The reproduced currents match the midlatitude Hall currents responsible for *PTKH*, as depicted in Figure 1. Figure 6c,d show the northward Hall and Pedersen currents, respectively. Both currents have the same direction as southward in the morning and northward in the afternoon and evening. The Hall current intensifies the Pedersen current near the dawn terminator, which is due to accumulation of electric charges at the terminator [47].

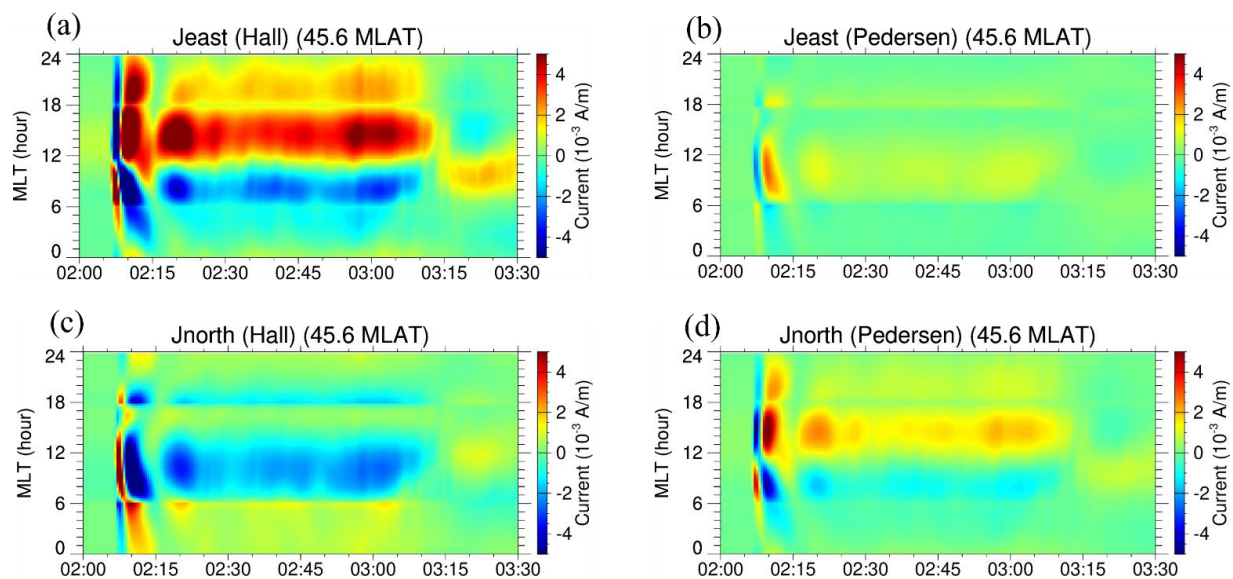


**Figure 6.** Ionospheric Hall and Pedersen currents at middle latitude ( $45.6^\circ$  magnetic latitude (MLAT)), reproduced by the REPPU global simulation model. (a, b) show eastward (westward) Hall and Pedersen currents in red (blue) color, respectively. (c,d) show northward (southward) Hall and Pedersen currents in red (blue) color, respectively. The vertical axis is the magnetic local time (MLT) and the horizontal axis is the simulation time (hh:mm).

Figure 7 shows the Hall and Pedersen currents at the latitude of OKI ( $17.0^\circ$  MLAT) and Pedersen (Cowling) current at the equator ( $0.0$  MLAT) in the same format as in Figure 6. Figure 7a,b show that the Hall current is westward in the morning and eastward in the afternoon and evening, which is larger than the Pedersen current density of which direction is eastward in the day. The reproduced currents match the extension of the Hall currents to low latitude consistent with the observations. Figure 7c,d show that the southward/northward Pedersen currents are dominant in the morning/afternoon, which are connected to the eastward Cowling current (*EEJ*) in the day (Figure 7e). The reproduced currents match the Pedersen-Cowling current circuit between the midlatitude and equator, consistent with the current circuit depicted in Figure 1. It should be noted that the regions of the eastward Cowling currents and northward Pedersen currents expand into the evening sector, which would reduce the Cowling and Pedersen current densities in the afternoon. *EEJ* has been shown to be maximum before noon [48], consistent with the reduced Cowling current density in the afternoon.

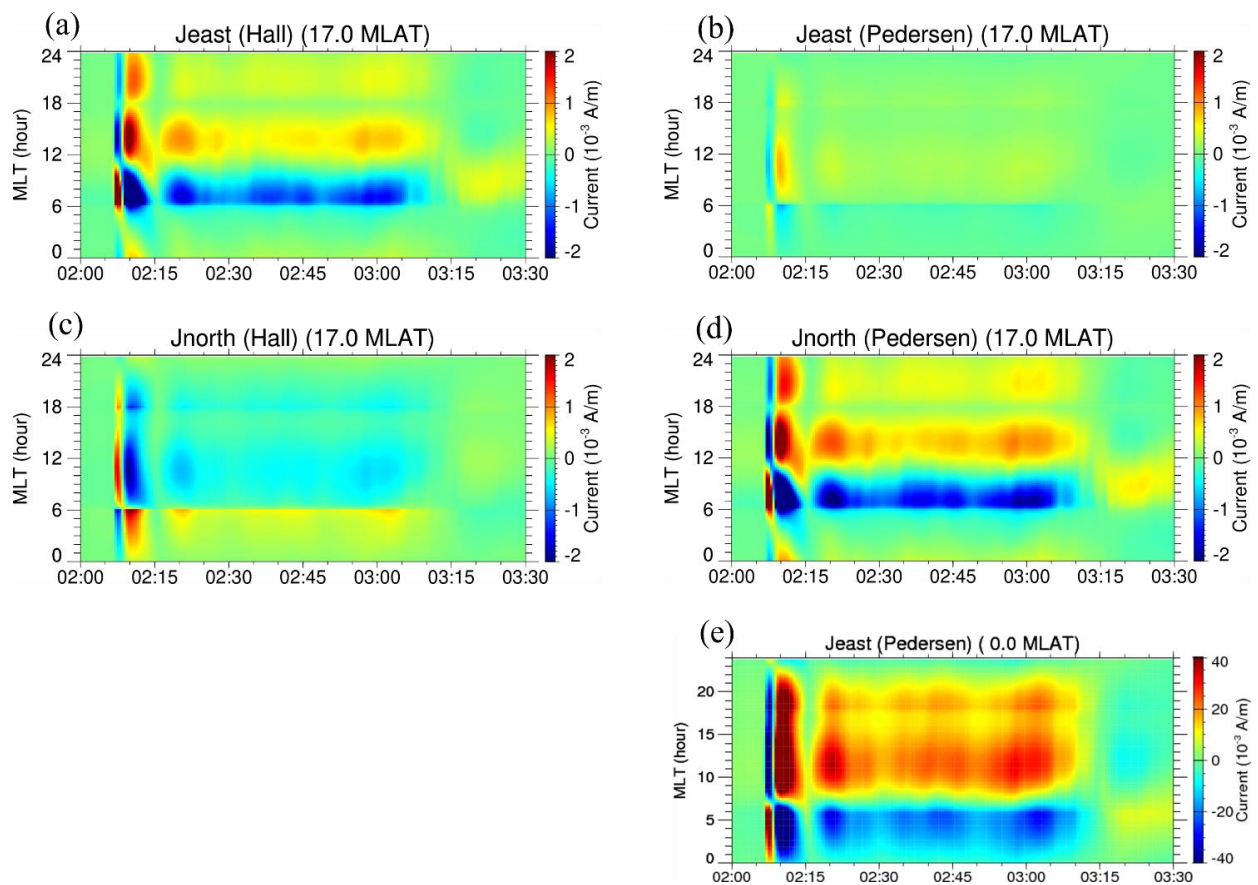


**Figure 7.** Ionospheric Hall and Pedersen currents at low latitude ( $17.0^\circ$  MLAT), and the equatorial Pedersen (Cowling) current, reproduced by the REPPU global simulation model. (a–d) are in the same format as (a–d) in Figure 6. (e) is in the same format as (b).

## 5. Summary and Discussion

We have analyzed DP2 events with negative correlations between  $PTKH$  and  $PTKD$  recorded at midlatitude,  $PTK$ , in the morning and afternoon sectors. We showed negative/positive correlations between  $PTKH$  and  $EEJ$  in the morning/afternoon and positive/negative correlations between  $PTKD$  and  $EEJ$  in the morning/afternoon. These results meet the DP2 current system created by the prompt penetration electric field (PPEF), which is composed of two-cell Hall current vortices surrounding the R1FACs and Pedersen-Cowling current circuits between the R1FACs and  $EEJ$ , as depicted in Figure 1. Although midlatitude magnetic fields are strongly affected by the magnetospheric currents, such as the magnetopause currents, ring currents, FACs, and so on, midlatitude magnetometers will detect the PPEF if we pick out DP2 events with negative correlations between  $H$  and  $D$ . The midlatitude  $D-EEJ$  relationship has been used to identify the PPEF of substorm [21] and geomagnetic storm [33]. The usefulness of the  $D-EEJ$  relationship has been confirmed by our analyses.

We here stress the important role of the Pedersen-Cowling current circuit in understanding geomagnetic and ionospheric disturbances at low and equatorial latitudes. As the Pedersen currents are carried by the  $TM_0/TEM$  mode waves in the Earth-ionosphere waveguide/transmission line [40], the Pedersen-Cowling current circuit is an energy channel from high latitude to the equator. Kikuchi [40] showed that the Poynting flux is transmitted at the speed of light in the space between the ground and ionospheric E-layer. A fraction of the Poynting flux penetrates into the ionospheric F-layer and further to the inner magnetosphere, which results in a quick response of the electric field and magnetic field disturbances at the equator [3,18,49] and inner magnetosphere [35,36].

We should recall that ground magnetic disturbances are caused by ionospheric currents and also by magnetospheric currents. If  $PTKH$  and  $OKIH$  were caused by magnetospheric currents in the equatorial plane of the magnetosphere like magnetopause and ring currents,  $OKIH$  should be larger than or almost comparable to  $PTKH$ . As we have shown in Figures 2 and 4,  $OKIH$  is smaller than  $PTKH$  and  $YAPH$ . Moreover,  $PTKH$  and some  $OKIH$  are in opposite polarity to  $EEJ$  in the morning sector, which is not consistent with the same polarity expected at low latitude and  $EEJ$  as caused by magnetospheric currents during SC [13] and solar wind-driven DP2 [7]. Thus,  $PTKH$  and  $YAPH$  are almost caused by ionospheric DP2 currents. Another candidate of the magnetospheric currents is FACs, but they make negative  $H$  at PTK and OKI when we observe positive  $EEJ$ . This FAC effect may be contained in the negative  $PTKH$  and  $OKIH$  in the morning, but its effect is negligibly small, because no such effects are observed in the afternoon sector. On the other hand, Kikuchi et al. [41] showed that the positive PI of SC occurs in the afternoon in winter, which is caused by positive magnetic fields due to the FACs dominating over the negative PI due to ionospheric currents. Imajo et al. [17] showed that the phase reversal in  $D$  of Pi2 pulsations occurs 0.5 h after sunrise and 2–3 h before sunset, which means that the FACs effects can overcome ionospheric currents late in the afternoon, as well as in the night. The lower values of  $cc(PTKD-EEJ)$  in the afternoon than in the morning may be due to contamination of FAC effects in  $PTKD$ . We suggest that the high correlations between  $H$  and  $D$  help identify the magnetic fields being caused by the DP2 currents.

Here, we raise a question one might have;  $H$  and  $D$  could be caused by a single Hall or Pedersen current with north-east or north-west direction. If the negative  $H$  and positive  $D$  in the morning were caused by a single Hall or Pedersen current, we would expect that the current flows south-westward. This direction does not meet the clockwise flow of the Hall current surrounding the FAC and does not meet the southward or south-eastward Pedersen current connecting to  $EEJ$ . Likewise, if the positive  $H$  and negative  $D$  in the afternoon were caused by a north-eastward current, it would be difficult to achieve a current circuit with  $EEJ$  that flow in the day and evening. Thus, it is reasonable to attribute the midlatitude  $H$  and  $D$  to the Hall and Pedersen currents, respectively, as depicted in Figure 1.

It is interesting to note that the Hall currents extend to low latitude, OKI (16.95° GML), where  $H$  is negative corresponding to positive  $EEJ$  (Figure 2a–c). We usually derive  $EEJ$  from  $YAPH$  subtracted by  $OKIH$ , by assuming that  $OKIH$  is not contributed by the ionospheric currents but totally caused by magnetospheric currents. The negative correlation between  $OKIH$  and  $YAPH / EEJ$  indicates that the westward Hall currents extend down to OKI, while  $YAPH$  is enhanced by the eastward Cowling currents. The contribution of the DP2 currents at OKI was found to be not negligible for the PI of SC [50]. They reported that PI appeared in 10–20% of the analyzed equatorial PI events. Our simulation results in Section 4 supports the extension of the Hall currents to the latitude of OKI. It should be stressed that the derivation of  $EEJ$  using  $OKIH$  as a reference does not make significant errors, since Hall current effects at OKI are much smaller than those of the Cowling currents.

Bay-like magnetic increases observed at middle latitudes have often been used as a signature of the eastward PPEF (e.g., Huang et al. [51]). Hashimoto et al. [32] pointed out that the midlatitude  $H$  used in Huang et al. [51] is suppressed or even negative at midlatitude during the period of positive  $EEJ$ . As we have shown in the present paper,  $PTKH$  and  $OKIH$  are negative in the morning when bay-like increases are observed in  $EEJ$  as in Figure 2a (2133UT). In Figure 2d, on the other hand,  $EEJ$  and  $OKIH$  are positive at 2240UT, but  $PTKH$  is negative, which is due to difference in the latitudinal dependence of the DP2 Hall currents. Hashimoto et al. [32] also pointed out that the amplitude of the bay-like increase in Huang et al. [51] does not show latitudinal change expected by DP2 currents in the afternoon sector. As we have shown in Figure 4,  $OKIH$  is much smaller than  $PTKH$ , corresponding to significant  $EEJ$ . The latitudinal dependence indicates strong contribution of the DP2 currents, consistent with the amplitude of DP2 decreasing steeply with decreasing latitude, but enhanced dramatically at the dayside equator [3]. If we have meridional chains of magnetometer, it would be easy to identify magnetic perturbations

caused by the PPEF. However, it would also be easy to identify the PPEF by examining  $H$ - $D$  correlations, even if we have only one station at midlatitude.

The high correlation between the midlatitude  $D$  and  $EEJ$  indicates achievement of the Pedersen–Cowling current circuit between midlatitude and equator, where the energy is transmitted by the  $TM_0$ /TEM mode in the Earth–ionosphere waveguide/transmission line [40]. The energy dissipated in  $EEJ$  should be supplied by a wave which propagates from the dynamo in the outer magnetosphere created by the solar wind–magnetosphere interaction [8–10]. There are two kinds of wave that transmits the energy to the ionosphere. One is the fast (compressional) mode with magnetic field parallel to the ambient magnetic field ( $B_0$ ), which propagates in the equatorial plane of the magnetosphere to middle and low latitude ionosphere. The second one is the transverse magnetic (TM) mode with the wave magnetic field perpendicular to the propagation plane containing the pair of FACs, which propagates to the polar ionosphere along  $B_0$  [52,53]. There have been lots of papers discussing that the fast mode wave supplies the PPEF responsible for geomagnetic and ionospheric perturbations at low latitude and equator (e.g., [54]). However, the electromagnetic energy is not discussed in the scenario of the fast mode propagation. In other words, the energy-consuming Pedersen/Cowling currents have not been explained by means of the fast mode wave. Tamao [52,53] attempted to explain the two-cell Hall current vortices of the PI of SC with the converted transverse mode (CT mode) that has been converted at the wave front of the fast mode, but the CT mode does not contain curl-free electric field, i.e., no FACs are supplied to the midlatitude ionosphere. Moreover, the fast mode wave does not compress the midlatitude ionosphere as observed by the HF Doppler sounder, which means that no energy is supplied to the ionosphere [30]. The conducting Earth also does not allow the compressional wave to survive in the ionosphere [55]. Contrast to the fast mode, the TM mode carries energy down to the polar ionosphere with the pair of FACs [52,53], and then to the equatorial ionosphere with the ionospheric Pedersen currents and ground surface currents in the Earth–ionosphere waveguide/transmission line [40,44]. The pair of field lines carrying the FACs works as a transmission line [56] and the Earth–ionosphere waveguide works as a lossy transmission line [40]. In the transmission line, the  $TM_0$  or TEM mode wave carries electromagnetic energy that are consumed in the Pedersen/Cowling currents. It should be stressed that the theory/model aiming for understanding fast propagation of electric and magnetic fields to low latitude ionosphere should also explain energy supply to the Pedersen and Cowling currents.

## 6. Conclusions

We picked out 39 DP2 events recorded at Paratunka, Russia (PTK, 45.58° N geomagnetic latitude (GML)) in the morning and 34 DP2 events in the afternoon, which are characterized by correlations,  $cc(PTKH-D) < -0.8$ . We found that all the events are associated with high  $cc(PTKD-EEJ)$  and  $cc(OKID-EEJ)$  with positive correlations in the morning and negative in the afternoon, meeting the Pedersen–Cowling current circuit from the R1FACs to  $EEJ$  through the Pedersen currents over the middle and low latitudes. The DP2 Hall currents extend down to low latitude OKI (16.95° GML), where the magnetospheric currents have been supposed to make major effects. As a result,  $OKIH$  is negatively correlated with  $EEJ$ . With these analyses, we conclude that the high  $cc(H-D)$  at middle latitudes can be used as a detector of the PPEF.

**Author Contributions:** T.K. and K.K.H. made magnetometer data analyses. T.T. performed global simulations of the DP2 currents. Y.N. provided ideas about similarities between DP2 currents and Pi2 pulsations. T.N. performed magnetometer operation. All authors have read and agreed to the published version of the manuscript.

**Funding:** This study is supported by the grants-in-aid for Scientific Research (15H05815, 20H01960) of Japan Society for the Promotion of Science (JSPS) and by JSPS KAKENHI grant number JP22540461 and JP26400481. The works of TK are supported by the joint research program of the Institute for Space–Earth Environmental Research, Nagoya University, the KDK of the Research Institute for Sustainable Humanosphere, Kyoto University, and National Institute of Polar Research, Tokyo. The works of YN is supported by NASA grant 80NSSC18K0657, 80NSSC20K0604, 80NSSC20K0725, 80NSSC21K1321 and 80NSSC20K1788, NSF grant AGS-1907698 and AGS-2100975, and AFOSR grant FA9559-16-1-0364.

**Institutional Review Board Statement:** Not applicable.

**Informed Consent Statement:** Not applicable.

**Data Availability Statement:** Magnetometer data at PTK, OKI, YAP are available on request from the corresponding author. The data are not publicly available due to that the data was collected for real-time space weather monitoring at the National Institute of Communications and Technology.

**Acknowledgments:** The results presented in this paper rely on the data collected at Paratunka, Okinawa, and Yap as the Space Weather Magnetometer Network by the National Institute of Communications and Technology (NICT). We thank the Institute of Cosmophysical Research and Radio Wave Propagation for Paratunka, Ryukyu University for Okinawa and NOAA National Weather Service for Yap.

**Conflicts of Interest:** The authors declare no conflict of interest.

## Abbreviations

SC	geomagnetic sudden commencement
PI	preliminary impulse
MI	main impulse
DL	stepwise low latitude magnetic disturbance
EEJ	equatorial electrojet
TM0	zeroth-order transverse magnetic
MHD	magnetohydrodynamic
REPPU	Reproduce Plasma Universe
GML	geomagnetic latitude
MLT	magnetic local time

## References

1. Nishida, A.; Iwasaki, N.; Nagata, T. The origin of fluctuations in the equatorial electrojet; A new type of geomagnetic variation. *Ann. Geophys.* **1966**, *22*, 478–484.
2. Nishida, A. Coherence of geomagnetic DP2 magnetic fluctuations with interplanetary magnetic variations. *J. Geophys. Res.* **1968**, *73*, 5549–5559. [[CrossRef](#)]
3. Kikuchi, T.; Lühr, H.; Kitamura, T.; Saka, O.; Schlegel, K. Direct penetration of the polar electric field to the equator during a DP2 event as detected by the auroral and equatorial magnetometer chains and the EISCAT radar. *J. Geophys. Res.* **1996**, *101*, 17161–17173. [[CrossRef](#)]
4. Kikuchi, T.; Ebihara, Y.; Hashimoto, K.K.; Kataoka, R.; Hori, T.; Watari, S.; Nishitani, N. Penetration of the convection and overshielding electric fields to the equatorial ionosphere during a quasiperiodic DP 2 geomagnetic fluctuation event. *J. Geophys. Res.* **2010**, *115*, A05209. [[CrossRef](#)]
5. Koba, A.T.; Amory-Mazaudier, C.; Do, J.M.; Luehr, H.; Hougoinou, E.; Vassal, J.; Blanc, E.; Curto, J.J. Equatorial electrojet as part of the global circuit: A case-study from the IEEY. *Ann. Geophys.* **1998**, *16*, 698–710. [[CrossRef](#)]
6. Koba, A.T.; Richmond, A.D.; Emery, B.A.; Peymirat, C.; Lühr, H.; Moretto, T.; Hairston, M.; Amory-Mazaudier, C. Electrodynamic coupling of high and low latitudes: Observations on May 27, 1993. *J. Geophys. Res.* **2000**, *105*, 22979–22989. [[CrossRef](#)]
7. Sibeck, D.G.; Takahashi, K.; Yumoto, K.; Reeves, G.D. Concerning the origin of signatures in dayside equatorial ground magnetograms. *J. Geophys. Res.* **1998**, *103*, 6763–6769. [[CrossRef](#)]
8. Tanaka, T. Generation mechanisms for magnetosphere-ionosphere current systems deduced from a three-dimensional MHD simulation of the solar wind-magnetosphere-ionosphere coupling processes. *J. Geophys. Res.* **1995**, *100*, 12057–12074. [[CrossRef](#)]
9. Fujita, S.; Tanaka, T.; Kikuchi, T.; Fujimoto, K.; Hosokawa, K.; Itonaga, M. A numerical simulation of the geomagnetic sudden commencement: 1. Generation of the field-aligned current associated with the preliminary impulse. *J. Geophys. Res.* **2003**, *108*, 1416. [[CrossRef](#)]

10. Fujita, S.; Tanaka, T.; Kikuchi, T.; Fujimoto, K.; Itonaga, M. A Numerical Simulation of the Geomagnetic Sudden Commencement: 2. Plasma Processes in the Main Impulse. *J. Geophys. Res.* **2003**, *108*, 1417. [[CrossRef](#)]
11. Hirono, M. A theory of diurnal magnetic variations in equatorial regions and conductivity of the ionosphere E region. *J. Geomag. Geoelectr. Kyoto* **1952**, *4*, 7–21. [[CrossRef](#)]
12. Baker, W.G.; Martyn, D.F. Electric currents in the ionosphere I. The conductivity. *Philos. Trans. R. Soc. London. Ser. A* **1953**, *246*, 281–294.
13. Araki, T. A physical model of the geomagnetic sudden commencement, Solar Wind Sources of Magnetospheric Ultra-Low-Frequency Waves. *Geophys. Monogr.* **1994**, *81*, 183–200.
14. Trivedi, N.B.; Arora, B.R.; Padilha, A.L.; da Costa, J.M.; Dutra, S.L.G.; Chamalaun, F.H.; Rigoti, A. Global Pc5 geomagnetic pulsations of March 24, 1991, as observed along the American sector. *Geophys. Res. Lett.* **1997**, *24*, 1683. [[CrossRef](#)]
15. Motoba, T.; Kikuchi, T.; Lühr, H.; Tachihara, H.; Kitamura, T.-I.; Hayashi, K.; Okuzawa, T. Global Pc5 caused by a DP2-type ionospheric current system. *J. Geophys. Res.* **2002**, *107*, A2. [[CrossRef](#)]
16. Shinohara, M.; Yumoto, K.; Yoshikawa, A.; Saka, O.; Solov'yev, S.I.; Vershinin, E.F.; Trivedi, N.B.; Da Costa, J.M. The 210 MM Magnetic Observation Group Wave characteristics of daytime and nighttime Pi2 pulsations at the equatorial and low latitudes. *Geophys. Res. Lett.* **1997**, *24*, 2279–2282. [[CrossRef](#)]
17. Imajo, S.; Yoshikawa, A.; Uozumi, T.; Ohtani, S.; Nakamizo, A.; Marshall, R.; Shevtsov, B.M.; Akulichev, V.A.; Sukhbaatar, U.; Liedloff, A.; et al. Pi2 pulsations observed around the dawn terminator. *J. Geophys. Res. Space Phys.* **2015**, *120*, 2088–2098. [[CrossRef](#)]
18. Rastogi, R.G. Geomagnetic storms and electric fields in the equatorial ionosphere. *Nature* **1977**, *268*, 422–424. [[CrossRef](#)]
19. Kikuchi, T.; Lühr, H.; Schlegel, K.; Tachihara, H.; Shinohara, M.; Kitamura, T.-I. Penetration of auroral electric fields to the equator during a substorm. *J. Geophys. Res.* **2000**, *105*, 23251–23261. [[CrossRef](#)]
20. Kikuchi, T.; Hashimoto, K.K.; Nozaki, K. Penetration of magnetospheric electric fields to the equator during a geomagnetic storm. *J. Geophys. Res.* **2008**, *113*, A06214. [[CrossRef](#)]
21. Hashimoto, K.K.; Kikuchi, T.; Watari, S.; Abdu, M.A. Polar-equatorial ionospheric currents driven by the region 2 field aligned currents at the onset of substorms. *J. Geophys. Res.* **2011**, *116*, A09217. [[CrossRef](#)]
22. Huang, C.-S. Statistical analysis of dayside equatorial ionospheric electric fields and electrojet currents produced by magnetospheric substorms during sawtooth events. *J. Geophys. Res.* **2012**, *117*, A02316. [[CrossRef](#)]
23. Yizengaw, E.; Moldwin, M.B.; Zesta, E.; Magoun, M.; Pradipta, R.; Biouele, C.M.; Rabiou, O.K.; Bamba, Z.; De Paula, E.R. Response of the equatorial ionosphere to the geomagnetic DP 2 current system. *Geophys. Res. Lett.* **2016**, *43*, 7364–7372. [[CrossRef](#)]
24. Zhang, K.; Wang, H.; Yamazaki, Y.; Xiong, C. Effects of subauroral polarization streams on the equatorial electrojet during the geomagnetic storm on June 1, 2013. *J. Geophys. Res. Space Phys.* **2021**, *126*, e2021JA029681. [[CrossRef](#)]
25. Zhang, K.; Wang, H.; Yamazaki, Y. Effects of subauroral polarization streams on the equatorial electrojet during the geomagnetic storm on 1 June 2013: 2. Temporal variations. *J. Geophys. Res. Space Phys.* **2022**, *127*, e2021JA030180. [[CrossRef](#)]
26. Yamazaki, Y.; Maute, A. Sq and EEJ—A review on the daily variation of the geomagnetic field caused by ionospheric dynamo currents. *Space Sci. Rev.* **2017**, *206*, 299–405. [[CrossRef](#)]
27. Wang, H.; Zheng, Z.; Zhang, K.; Wang, W. Influence of nonmigrating tides and geomagnetic field geometry on the diurnal and longitudinal variations of the equatorial electrojet. *J. Geophys. Res. Space Phys.* **2020**, *125*, e2019JA027631. [[CrossRef](#)]
28. Yamazaki, Y.; Harding, B.J.; Stolle, C.; Matzka, J. Neutral wind profiles during periods of eastward and westward equatorial electrojet. *Geophys. Res. Lett.* **2021**, *48*, e2021GL093567. [[CrossRef](#)]
29. Kikuchi, T.; Araki, T.; Maeda, H.; Maekawa, K. Transmission of polar electric fields to the Equator. *Nature* **1978**, *273*, 650–651. [[CrossRef](#)]
30. Kikuchi, T.; Hashimoto, K.K.; Tomizawa, I.; Ebihara, Y.; Nishimura, Y.; Araki, T.; Shinbori, A.; Veenadhari, B.; Tanaka, T.; Nagatsuma, T. Response of the incompressible ionosphere to the compression of the magnetosphere during the geomagnetic sudden commencements. *J. Geophys. Res. Space Phys.* **2016**, *121*, 1536–1556. [[CrossRef](#)]
31. Kikuchi, T.; Chum, J.; Tomizawa, I.; Hashimoto, K.K.; Hosokawa, K.; Ebihara, Y.; Hozumi, K.; Supnithi, P. Penetration of the electric fields of the geomagnetic sudden commencement over the globe as observed with the HF Doppler sounders and magnetometers. *Earth Planets Space* **2021**, *73*, 1–13. [[CrossRef](#)]
32. Hashimoto, K.K.; Kikuchi, T.; Tomizawa, I.; Nagatsuma, T. Substorm overshielding electric field at low latitude on the nightside as observed by the HF Doppler sounder and magnetometers. *J. Geophys. Res. Space Phys.* **2017**, *122*. [[CrossRef](#)]
33. Hashimoto, K.K.; Kikuchi, T.; Tomizawa, I.; Hosokawa, K.; Chum, J.; Buresova, D.; Nose, M.; Koga, K. Penetration electric fields observed at middle and low latitudes during the 22 June 2015 geomagnetic storm. *Earth Planets Space* **2020**, *72*, 1–15. [[CrossRef](#)]
34. Abdu, M.A.; Sastri, J.H.; Lühr, H.; Tachihara, H.; Kitamura, T.; Trivedi, N.B.; Sobral, J.H.A. DP 2 electric field fluctuations in the dusk-time dip equatorial ionosphere. *Geophys. Res. Lett.* **1998**, *25*, 1511–1514. [[CrossRef](#)]
35. Nishimura, Y.; Kikuchi, T.; Wygant, J.; Shinbori, A.; Ono, T.; Matsuoaka, A.; Nagatsuma, T.; Brautigam, D. Response of convection electric fields in the magnetosphere to IMF orientation change. *J. Geophys. Res.* **2009**, *114*, A09206. [[CrossRef](#)]
36. Nishimura, Y.; Kikuchi, T.; Shinbori, A.; Wygant, J.; Tsuji, Y.; Hori, T.; Ono, T.; Fujita, S.; Tanaka, T. Direct measurements of the Poynting flux associated with convection electric fields in the magnetosphere. *J. Geophys. Res.* **2010**, *115*, A12212. [[CrossRef](#)]
37. Araki, T. Global structure of geomagnetic sudden commencements. *Planet. Space Sci.* **1977**, *25*, 373–384. [[CrossRef](#)]

38. Kikuchi, T. Evidence of transmission of polar electric fields to the low latitude at times of geomagnetic sudden commencements *J. Geophys. Res.* **1986**, *91*, 3101–3105. [[CrossRef](#)]
39. Kikuchi, T.; Araki, T. Horizontal transmission of the polar electric field to the equator. *J. Atmos. Terr. Phys.* **1979**, *41*, 927–936. [[CrossRef](#)]
40. Kikuchi, T. Transmission line model for the near-instantaneous transmission of the ionospheric electric field and currents to the equator. *J. Geophys. Res. Space Phys.* **2014**, *119*, 1131–1156. [[CrossRef](#)]
41. Kikuchi, T.; Tsunomura, S.; Hashimoto, K.; Nozaki, K. Field-aligned current effects on midlatitude geomagnetic sudden commencements. *J. Geophys. Res.* **2001**, *106*, 15–555. [[CrossRef](#)]
42. Tsunomura, S. Characteristics of geomagnetic sudden commencement observed in middle and low latitudes. *Earth Planets Space* **1998**, *50*, 755–772. [[CrossRef](#)]
43. Tanaka, T. Magnetosphere-ionosphere convection as a compound system. *Space Sci. Rev.* **2007**, *133*, 1–72. [[CrossRef](#)]
44. Kikuchi, T. *Penetration of the Magnetospheric Electric Fields to the Low Latitude Ionosphere, Space Physics and Aeronomy Collection Volume 3: Ionosphere Dynamics and Applications, Geophysical Monograph 260*, 1st ed.; Huang, C., Lu, G., Eds.; John Wiley & Sons Inc.: Hoboken, NJ, USA, 2021. [[CrossRef](#)]
45. Tanaka, T.; Nakamizo, A.; Yoshikawa, A.; Fujita, S.; Shinagawa, H.; Shimazu, H.; Kikuchi, T.; Hashimoto, K.K. Substorm convection and current system deduced from the global simulation. *J. Geophys. Res.* **2010**, *115*, A05220. [[CrossRef](#)]
46. Ebihara, Y.; Tanaka, T.; Kikuchi, T. Counter equatorial electrojet and overshielding after substorm onset: Global MHD simulation study. *J. Geophys. Res. Space Phys.* **2014**, *119*. [[CrossRef](#)]
47. Wolf, R.A. Effects of ionospheric conductivity on convective flow of plasma in the magnetosphere. *J. Geophys. Res.* **1970**, *75*, 4677–4698. [[CrossRef](#)]
48. Lühr, H.; Rother, M.; Häusler, K.; Alken, P.; Maus, S. The influence of nonmigrating tides on the longitudinal variation of the equatorial electrojet. *J. Geophys. Res.* **2008**, *113*, A08313. [[CrossRef](#)]
49. Fejer, B.G.; Gonzales, A.C.; Farley, D.T.; Kelley, M.C.; Woodman, R.F. Equatorial electric fields during magnetically disturbed conditions 1. The effect of the interplanetary magnetic field. *J. Geophys. Res.* **1979**, *84*, 5797–5802. [[CrossRef](#)]
50. Shinbori, A.; Tsuji, Y.; Kikuchi, T.; Araki, T.; Watari, S. Magnetic latitude and local time dependence of the amplitude of geomagnetic sudden commencements. *J. Geophys. Res.* **2009**, *114*, A04217. [[CrossRef](#)]
51. Huang, C.-S.; Foster, J.C.; Goncharenko, L.P.; Reeves, G.D.; Chau, J.L.; Yumoto, K.; Kitamura, K. Variations of low-latitude geomagnetic fields and Dst index caused by magnetospheric substorms. *J. Geophys. Res.* **2004**, *109*, A05219. [[CrossRef](#)]
52. Tamao, T. The structure of three-dimensional hydromagnetic waves in a uniform cold plasma. *J. Geomagn. Geoelectr.* **1964**, *48*, 89–114. [[CrossRef](#)]
53. Tamao, T. Hydromagnetic interpretation of geomagnetic SSC\*. *Rep. Ionos. Space Res. Jpn.* **1964**, *18*, 16–31.
54. Tu, J.; Song, P. On the momentum transfer from polar to equatorial ionosphere. *J. Geophys. Res. Space Phys.* **2019**, *124*, 6064–6073. [[CrossRef](#)]
55. Kivelson, M.G.; Southwood, D.J. Hydromagnetic waves and the ionosphere. *Geophys. Res. Lett.* **1988**, *15*, 1271–1274. [[CrossRef](#)]
56. Sato, T.; Iijima, T. Primary sources of large-scale Birkeland currents. *Space Sci. Rev.* **1979**, *24*, 347–366. [[CrossRef](#)]